In vivo seamless genetic engineering via CRISPR-triggered single-strand annealing

Gustavo Aguilar[1†], Milena Bauer[1†], M. Alessandra Vigano[1], Carlos Jiménez-Jiménez[2], Isabel Guerrero[2], Markus Affolter[1].

1. Growth & Development, Biozentrum, Spitalstrasse 41, University of Basel, 4056 Basel, Switzerland.

2. Tissue and Organ Homeostasis, Centro de Biología Molecular "Severo Ochoa" (CSIC-UAM), Nicolás Cabrera 1, Universidad Autónoma de Madrid, Madrid, Spain.

† These authors contributed equally.

Keywords:
CRISPR, Cas9, Knock-in, SSA, Somatic, Drosophila, SEED, Harvest

Abstract

Precise genome engineering is essential for both basic and applied research, permitting the manipulation of genes and gene products in predictable ways. The irruption of the CRISPR/Cas technology accelerated the speed and ease by which defined exogenous sequences are integrated into specific loci. To this day, a number of strategies permit gene manipulation. Nevertheless, knock-in generation in multicellular animals remains challenging, partially due to the complexity of insertion screening. Even when achieved, the analysis of protein localization can still be unfeasible in highly packed tissues, where spatial and temporal control of gene labeling would be ideal. Here, we propose an efficient method based on homology-directed repair (HDR) and single-strand annealing (SSA) repair pathways. In this method, HDR mediates the integration of a switchable cassette. Upon a subsequent CRISPR-triggered repair event, resolved by SSA, the cassette is seamlessly removed. By engineering the Hedgehog (Hh) pathway components, we demonstrated fast and robust knock-in generation with both fluorescent proteins and short protein tags in tandem. The use of homology arms as short as 30 base pairs further simplified and cheapened the process. In addition, SSA can be triggered in somatic cells, permitting conditional gene labeling in different tissues. Finally, to achieve conditional labeling and manipulation of proteins tagged with short protein tags, we have further developed a toolbox based on rational engineering and functionalization of the ALFA nanobody.

Significance statement

CRISPR/Cas9 has revolutionized genome editing. However, seamless editing in multicellular organisms still presents many challenges, mainly derived from insertion screening. The tool we have developed permits fast, robust and cheap gene editing mediated by the SSA repair pathway. This pathway is highly conserved in different animal species; hence the methodology is a promising alternative for gene editing across organisms. We demonstrate that this approach can be used to achieve spatio-temporal control of gene-labeling, mediated by somatic Cas9 expression. This addition to the CRISPR repertoire opens a new avenue for the study of protein function and distribution, alone or in combination with other CRISPR based technologies. We further engineered a nanobody-based toolbox that permits precise manipulation and visualization of the generated knock-ins.

Introduction

Historically, genetic studies relied on randomly generated mutations. The analysis of these mutants paved the way to the enormous success of genetics in the last hundred years. However, as early as the 1980s (Smithies, Gregg, Boggs, Koralewski, & Kucherlapati, 1985), efforts have been devoted to obtain *ad hoc* gene engineering, and thus, rational manipulation of gene products. Today, the precise genomic insertion of exogenous sequences is critical for biological studies in all systems. Among other applications, it has permitted the generation of conditional gene knock-outs, gene tagging, and precise base-pair substitutions. Efficient generation of knock-ins has also an immediate application in gene therapy, where it has been successfully employed to correct pathogenic gene variants (DeWitt et al., 2016; Park et al., 2019). Hence, the development and implementation of efficient and precise knock-in techniques is, more than ever, urging.

The proposal of CRISPR/Cas as a gene-editing tool (Jinek et al., 2012) revolutionized the generation of knock-ins, both in terms of ease and precision. Briefly, CRISPR/Cas is used to generate double strand breaks (DSB) in a target locus, triggering the DNA's repair machinery. An exogenous DNA containing the intended insertion is provided to be used as a repair template during the process (Ceccaldi, Rondinelli, & D'Andrea, 2016). With some exceptions, Homology-directed repair (HDR) is the preferred pathway used to generate knock-ins (Bollen, Post, Koo, & Snippert, 2018). HDR rates are often low *in vivo* (Johnson & Jasin, 2000; Mao, Bozzella, Seluanov, & Gorbunova, 2008), thus, an efficient way for screening correct insertions is required.

Positive knock-in screening

To facilitate the screening, two-step knock-in approaches have grown increasingly popular, especially when editing multicellular organisms. In these cases, a selectable marker is inserted along with the desired element. After screening, the marker is removed by recombination via Cre/LoxP or Flipase/FRT systems (Bollen et al., 2018), resulting in scars of variable size. Although sometimes innocuous, these scars are generally incompatible with precise, in-frame protein tagging. As an alternative, piggyBac (PBac) techniques allow seamless marker removal (Yusa, 2013). This approach depends on the presence of a natural TTAA site around the insertion point or the engineering of such a site. PBac also requires targeted expression of a transposase and entails the risk of reintegration in other genomic locations (Ye et al., 2014).

Recently, approaches based on Microhomology-dependent End-Joining (MMEJ) have been proposed to seamlessly remove a marker from an engineered locus in iPSC cells (Kim et al., 2018; Roberts et al., 2019). In these approaches, the marker is flanked by guide RNA (gRNA) targets at both sides, cleavable by CRISPR. To favor MMEJ, small repeats (up to 50bp) are inserted at both sides of the gRNA targets. This strategy has been employed in cultured cells to create point mutations or insert fluorescent tags, where it has reached an efficiency of up to 50% (Roberts et al., 2019). The solely need of CRISPR/Cas makes this approach ideal for gene editing in multicellular organisms. Despite the suitability of the method, to our knowledge no reports on animals edited with such an approach have been published.

Another popular approach for gene editing involves the CRISPR-mediated insertion of *attP* sites (Baena-Lopez, Alexandre, Mitchell, Pasakarnis, & Vincent, 2013; Huang, Zhou, Dong, Watson, & Hong, 2009). *attP* provides a landing site into which *attB*-containing DNA can be

inserted. Although robust and modular, this approach involves several rounds of insertion and marker removal, with the concomitant increase in time. In Drosophila, these methodologies often involve several rounds of injection and can take more than 10 generations, complicating its implementation in vertebrates.

Spatio-temporal control of gene labeling

When achieved, endogenous tagging permits both the visualization and the manipulation of the targeted gene product. Nonetheless, visualization of the protein of interest may remain limited when studding highly-packed tissues, like the brain. To overcome these limitations, genetic engineering that permits endogenous tagging in a distinct subset of cells has been proposed (Alexandre, Baena-Lopez, & Vincent, 2014; Baena-Lopez et al., 2013; Koles, Yeh, & Rodal, 2015). Such approaches require up to four integration/excision events (Baena-Lopez et al., 2013), making its application in vertebrates costly and time consuming, and consequently, such approaches remain rare. Moreover, these approaches require the implementation of an increasingly complex genetic toolbox, lacking in most species.

To overcome these problems, protein-based methods have been developed to selectively label specific cells. In some cases, the gene of interest is tagged with a split version of GFP (He, Cuentas-Condori, & Miller, 2019; R. Kamiyama et al., 2021). Only when the complementary portion of GFP is expressed, the fluorescent signal is reconstituted and the protein can be visualized. The main limitation of these technologies is the necessity of specific alleles, solely generated for this purpose.

Nanobody-based tools also permit the visualization of proteins in specific cells. In this case, nanobodies recognizing the targeted protein or an attached fluorescent moiety have been used (Helma et al., 2012; D. Kamiyama et al., 2015; Panza, Maier, Schmees, Rothbauer, & Soellner, 2015). Their implementation remains limited at the moment, due either to the cost and complexity of raising specific nanobodies or to the background signal that some of them might display when expressed (Aguilar, Vigano, Affolter, & Matsuda, 2019).

In order to tackle limitations in time, cost and efficiency, we propose a two-step approach to rapidly and robustly generate knock-ins in *Drosophila melanogaster*. The technique, named SEED (from "**S**carless **E**diting by **E**lement **D**eletion"), relies only on CRISPR/Cas for both steps. SEED exploits HDR and Single stranded annealing (SSA) repair pathways to insert and seamlessly remove the cassette, respectively. SEED provides a fast, robust and cheap alternative for current tagging methods. The high efficiency of removal permits somatic gene labeling, mediated by the expression of Cas9. This is the first example of lineage-restricted endogenous tagging mediated by CRISPR/Cas. Combination of the SEED technology with other tissue-specific CRISPR applications opens the way for novel experimental avenues, such as protein localization screenings. To further enhance the usefulness of this technology, we have also developed a novel nanobody-based toolbox to manipulate gene products tagged with ALFA-tag (Götzke et al., 2019). To do so, we have rationally engineered and functionalized the anti-ALFA nanobody, permitting protein visualization, degradation or hinderance of secretion.

Results

SEED/Harvest: Generation of scarless genome insertions via a combination of HDR and SSA repair pathways

We envisioned a scarless knock-in strategy that makes use of the SSA pathway. SSA is a highly conserved repair pathway, strongly preferred when repeated sequences flank the DSB (Bhargava, Onyango, & Stark, 2016; Preston, Engels, & Flores, 2002). In our approach, a cassette is incorporated in the gene of interest via CRISPR-triggered HDR (Figure 1A). The cassette consists of a selectable marker, flanked by the target sequences of two gRNAs with no cutting sites anywhere else in the genome (here named gRNAs #1 and #2) (Garcia-Marques et al., 2019). Flanking these sites, the exogenous sequence to be inserted is split in a 5' and a 3' parts, sharing a repeated sequence of 100bp to 400bp. The SEED cassette is then flanked by the 5' and 3' homology arms required for HDR-mediated insertion. In order to trigger plasmid linearization *in vivo*, the target sequences of the gRNA used to generate the genomic DSB are added flanking the whole construct. After insertion and screening, the marker is seamlessly removed by a subsequent CRISPR-triggered repair event, resolved by SSA (Figure 1B). In this step, the repeats anneal and the region in-between is removed, resulting in a scarless knock-in (Figure 1C). Our strategy was inspired by the recently developed CRISPR-triggered cell-labeling (Garcia-Marques et al., 2019) and has a pilot precedent in cell culture (Li et al., 2018).

To facilitate cassette removal and selection, we generated flies containing a balancer chromosome bearing both ubiquitously expressed gRNAs #1 and #2 and a germ line-driven Cas9 (*nos-Cas9, U6-gRNA#1+2*), hereafter named "Harvester" (Supplementary Figure 1A, B). Harvester stocks permit the generation and selection of rearranged transgenes in one and a half months (Supp Figure 1D).

In order to quantitatively test the efficiency of the SSA-mediated rearrangement *in vivo*, we generated a construct containing a sfGFP-SEED cassette downstream of UAS sequences (*UAS-sfGFP-SEED*) and inserted it in the *attP*86Fb landing site via integrase-mediated insertion. *UAS-sfGFP-SEED* flies displayed easily recognizable dsRED signal across different stages (Figure 1D). When un-cleaved, expression of *UAS-sfGFP-SEED* results in a non-fluorescent truncated sfGFP protein, due to a stop codon immediately before the 3xP3-FP marker. Only in those cases in which the targeted locus undergoes SSA, the full sfGFP coding sequence is reconstituted. We analyzed the progeny of *Harvester*/*UAS-sfGFP-SEED* flies crossed with the ubiquitous *Act5C*-Gal4 driver (Figure 1E, crossing scheme in Supp Figure 1C). Of those flies that inherited the *UAS-sfGFP-SEED* insertion, most of the progeny expressed GFP (87.8%). Among the GFP-negative flies, half of them still kept the 3xP3-dsRED marker, permitting their sorting. Thus, 94.8% of the flies that lost the marker underwent seamless rearrangement. In addition, we tested the efficiency of the ALFA:HA-SEED harvesting. Despite the shorter repeat (100bp), in 67% of the cases, SSA happened seamlessly when 3xP3-dsRED was removed (Figure 1E).

We then generated a customized library of SEED cassettes (Figure 1F) ready to insert either popular fluorescent proteins (sfGFP, mCherry, EYFP:HA) or short protein tags in tandem (ALFA-tag, HA-tag, MoonTag and OLLAS-tag). Since dsRED and mCherry share long stretches of sequence that might interfere during SSA repair, the 3xP3-dsRED of pSEED-mCherry plasmid was substituted for 3xP3-GFP. For all the chosen proteins, highly selective antibodies are available as well as high-affinity protein binders that enable *in vivo* manipulation (Aguilar et al., 2019). In addition to tagging reagents, we generated a pSEED-

T2A-GAL4 plasmid that allows rapid generation of Gal4 driver lines, and an empty SEED vector, permitting *ad hoc* gene manipulation.

Precise gene tagging using SEED technology

As a proof of principle, we attempted the tagging of the *patched* (*ptc*) and the *spaghetti squash* (*sqh*) genes with the pSEED-ALFA:HA donor plasmid. In both cases, gRNAs and Cas9 were provided by integrated transgenes, as this approach has been shown to result in enhanced integration efficiency (Port, Chen, Lee, & Bullock, 2014a). Long homology arms (~1.4kb) where used flanking the cassettes (Figure 2A, B). High rates of insertion in the germ cells were observed, with 58% (*ptc*) and 50% (*sqh*) of the F0 parents giving rise to progeny positive for the 3xP3 marker. Seamless SEED cassette removal occurred in similar rates as for *UAS-ALFA:HA-SEED*. Immunostaining of Ptc::ALFA:HA permitted simultaneous visualization of both tags using anti-HA monoclonal antibody and fluorescently conjugated anti-ALFA nanobody (Figure 2C). Ptc was detected along the antero-posterior (AP) boundary, in a characteristic anterior stripe (Capdevila, Estrada, Sanchezherrero, & Guerrero, 1994). Sqh was detected in all cells, decorating the cellular cortex (Figure 2D, E).

Often, one of the main limiting steps in the generation of knock-ins is the construction of donor plasmids. Amplification and cloning of long homology arms can hamper transgene generation. To increase cloning speed and efficiency, we adopted the use of short homology arms (<200bp) (Kanca et al., 2019). This strategy permits the cheap (around 80€ by the time this manuscript is written) synthesis of vectors including homology arms, into which the SEED cassette can be added in a one-day cloning (Supplementary Figure 2A, see material and methods). Using this strategy, we tagged the genes of the Hh pathway components *interference hedgehog* (*ihog*), *brother of ihog* (*boi*) and *shifted* (*shf*). (Figure 2F, G, H). Instead of using genetically provided gRNAs, we co-injected gRNA expressing plasmids together with our donors. The strategy resulted in a similar integration efficiency as that observed in the *ptc* locus employing long homology arms and genetically provided gRNAs (Figure 2A). For all the knock-ins we generated, the corresponding expression patterns mimicked that of antibodies described in the literature (Figure 2C, D, I, J, K) (Bilioni et al., 2013; Glise et al., 2005; Yan et al., 2010) and all resulted in functional variants, presenting no obvious mutant phenotypes (data not shown).

Recent studies have proposed the integration of transgenes employing much shorter homology arms, exploiting either the Micro-Homology End Joining (MHEJ) (Nakade et al., 2014; Sakuma, Nakade, Sakane, Suzuki, & Yamamoto, 2016) or more generally homologous-mediated end joining (HMEJ) (Yao et al., 2018) pathways. MHEJ can support transgene integration with sequences as short as 5bp. Since the use of such homology arms could further simplify the generation of the donor, we generated a pSEED-mCherry donor vector bearing 30bp homology arms for the *boi* locus. Thus, donor plasmids could be easily generated in a one-day cloning (Supplementary figure 2B). Insertion point and gRNAs were identical to those employed in figure 2G, and therefore, can be directly compared. The percentage of founders was 41% (Figure 2L), which only represented a slight decrease respect the 63% using donors with 185bp homology arms. On the other hand, the use of such short homology arms resulted in a decrease of the precision with which the transgenes are integrated: while 185bp resulted in 100% accuracy, using 30bp resulted in 60% of the

founders containing accurate insertions (Figure 2M). Together, our data suggests that MHEJ-dependent knock-ins represent a promising alternative to HDR in Drosophila.

Generation of point mutations via SEED/Harvest

In many occasions, especially in gene therapy, the intended genetic manipulation involves not the addition of a tag, but the mutation of one or several base-pairs. With slight modifications, SEED/Harvest can achieve the generation of point mutants. When not introducing a tag, the repeat used for SSA-mediated harvesting has to be introduced during the cloning, matching the endogenous sequence. This approached has been proven efficient in cell culture {Li, 2018 #527}, but its application *in vivo* remains unexplored. As a proof of principle, we have recently generated a point mutant in the *scalloped* (*sd*) locus using SEED/harvest (Mesrouze et al., 2022) (Supplementary figure 3A). In this case, the region to be mutated was duplicated at both sides of the SEED cassette (Supplementary Figure 3B). These repeats, of approximately 100 bp, contained the point mutation and silent mutations to avoid donor cutting by the gRNAs. The HDR mediated insertion resulted in a high number of dsRED positive animals (52%, n=33). Furthermore, we could harvest the SEED to generate the clean mutant (Supplementary Figure 3C).

CRISPR-triggered lineage-specific endogenous labeling.

One of the main limitations of endogenous labeling when studying protein localization is the widespread distribution of many proteins. This turns out to be particularly critical in tissues with an intricated three-dimensional structure, such as the brain, where linage-specific endogenous labeling would be most useful. In order to obtain tissue-specific protein labeling, the most common strategy is the overexpression of a tagged cDNA. Such approaches result in high amounts of protein being synthesized, with the risk of altering protein function and localization. As mentioned before, both sfGFP-SEED and mCherry-SEED cassettes are designed to produce a truncated non-fluorescent protein unless cleaved. We hypothesized that these cassettes could be used as switches in somatic cells, responsive to the presence of Cas9 and the gRNAs (Figure 3A). As a proof of principle, we attempted to activate the *ihog*$^{\text{sfGFP-SEED}}$ allele in wing disc cells. To do so, we provided Cas9 with a *hh*-Cas9 line and ubiquitously expressed gRNAs (*U6*-gRNA#1+2*)*. In the wing imaginal disc, *hh*-Cas9 is known to be expressed at high levels in the posterior compartment, and at low levels in the anterior. Crossing this line with reporters of CRISPR activity resulted in robust labeling of posterior compartment cells and sparse labeling in the anterior (Koreman et al., 2021). In our case, Ihog::sfGFP was reconstituted mainly in the anterior compartment, displaying few Ihog::sfGFP positive clones in the posterior (Figure 3B). This demonstrate the capacity of SEED cassettes to be rearranged in somatic cells, but also indicates that rearrangement requires low Cas9 levels. To confirm that this property is not exclusive to SEED, but general for SSA-dependent rearrangements, we used *hh*-Cas9 to trigger cell labeling using the recently generated CaSSA membrane reporters (Garcia-Marques et al., 2019). CaSSA reporters are also based on the reconstitution of a fluorescent protein via CRISPR-triggered SSA and have been widely validated for neuronal labeling in the brain (Garcia-Marques et al., 2019). Indeed, the Actin5C-CAAX-mCher(#2)rry CaSSA reporter using *hh*-Cas9 showed an activation pattern highly similar to that of Ihog:sfGFP (Supplementary figure 4A), confirming that SSA-dependent rearrangements are highly sensitive to Cas9 levels.

Interestingly, *ihog*$^{\text{sfGFP-SEED}}$ could also be activated in a similar pattern when using only the gRNA#2 (Supplementary figure 4B).

In order to demonstrate the capacity of Cas9 to direct endogenous labeling in other tissues, we activated the *ihog*$^{\text{sfGFP-SEED}}$ cassette using the neuronal lines *elav*-Cas9 and *vGlut*-Cas9 (Supplementary figure 4C, D). In both cases, labeling was easily detected in neural somas along the ventral nerval chord (VNC) of third instar larvae, indicating the feasibility of using this approach in the brain. Interestingly, activation of *ihog*$^{\text{sfGFP-SEED}}$ using elav-Cas9 resulted in large Ihog::sfGFP clones in the wing disc (Supplementary figure 4E), as the *elav* promoter has been shown to be transiently active at low levels in epithelial cells (Casas-Tintó, Arnés, & Ferrús, 2017).

In recent years, somatic expression of Cas9 has been proposed to exert different types of functions, such as gene knock-out (Meltzer et al., 2019; Port & Bullock, 2016; Port et al., 2020) or to positively or negatively label cells (Garcia-Marques et al., 2019; Koreman et al., 2021). In principle, the SEED technology can be easily used in combination with these technologies. To facilitate its use together with CaSSA reporters (Garcia-Marques et al., 2019), the gRNA targets used to activate SEED cassettes and CaSSA reporters are the same. We have previously shown that Ihog overexpression results in strong basolateral localization, leading to stabilization of filopodia emanating from Ihog-overexpressing cells (Bilioni et al., 2013; Bischoff et al., 2013; González-Méndez, Seijo-Barandiarán, & Guerrero, 2017; Simon et al., 2021). Localization of endogenous Ihog in filopodia could hardly be assessed by antibody staining, given its widespread distribution in the tissue. By combining *ihog*$^{\text{sfGFP-SEED}}$ and the Actin5C-CAAX-mCher(#2)rry reporter (Figure 3C), we labeled both Ihog and cell membranes when Cas9 was present in the same cells (Figure 3D). When the filopodia survived the fixation process, Ihog::sfGFP positive puncta could be observed in these basal structures (Figure 3E).

One of the limitations of combining SEED cassettes with CaSSA reporters for restricted labeling of brain cells is the presence of the 3xP3-FP marker. The 3xP3 enhancer drives expression in numerous tissues throughout development, especially in the brain and the eyes (Figure 1D) (Horn, Jaunich, & Wimmer, 2000), impeding simultaneous cell-labeling and endogenous gene tagging. To overcome this limitation, we designed a SEED cassette (*SEED-LoxP*) that permits Cre-mediated removal of the 3xP3 marker prior to harvesting (Supplementary figure 4F, G). Using this approach, we generated an *ihog*$^{\text{sfGFP-SEED-LoxP}}$ allele. The knock-in efficiency using this donor was similar to that obtained for *ihog*$^{\text{sfGFP-SEED}}$ (Supplementary figure 4H).

Conditional rescue of mutant SEED alleles

When SEED cassettes are first inserted in the 5' or internal positions of a gene, the coding region will be abruptly interrupted after the first repeat of the cassette, potentially generating a mutant. We envisioned that in these cases, the mutants could be rescued by conditional expression of Cas9 and harvesting gRNAs.

To test this possibility, we analyzed the *shf*$^{\text{sfGFP-SEED}}$ allele produced during *shf*^{sfGFP} generation (Figure 2H). Shf is a highly diffusible factor strictly required for Hh dispersal in Drosophila (Glise et al., 2005; Gorfinkiel, Sierra, Callejo, Ibanez, & Guerrero, 2005) SEED insertion is predicted to generate a truncated protein only preserving the first 60 amino acids of Shf. Indeed, *shf*$^{\text{sfGFP-SEED}}$ gave rise to the same phenotype as the previously reported *shf* null alleles (Lindsley & Zimm, 1992), displaying strong reduction of the intervein territory

between veins 3 and 4 of the wing (Figure 3F). Accordingly, the range of Hh signaling, determined by the Hh targets Ptc and Ci155, was dramatically affected (Figure 3F, H). When *shf*$^{sfGFP\text{-}SEED}$ was combined with *hh*-Cas9 and gRNAs targeting the SEED, both wild type wing phenotype and Hh signaling range were partially restored (Figure 3G, H, I). Interestingly, GFP::Shf protein was detected in both posterior and anterior compartments. This result is consistent with previous reports, that found a non-autonomous effect of Shf since it disperses across large territories (Glise et al., 2005; Gorfinkiel et al., 2005; Sanchez-Hernandez, Sierra, Ramalho Ortigao-Farias, & Guerrero, 2012). Thus, SEED cassettes can be efficiently used to generate conditional rescue experiments.

Nanobody-based visualization and manipulation of proteins tagged with short peptide tags placed in tandem.

SEED cassettes permit the restricted labeling of endogenously proteins with mCherry and GFP. However, because of their length, SEED cassettes bearing short peptide tags cannot be conditionally activated. We planned an alternative to visualize such knock-ins via a chromobody against the ALFA peptide. Chromobodies are fusion proteins between a protein binder and a fluorescent protein. We and others have developed similar tools in *Drosophila* (D. Kamiyama et al., 2015; Vigano et al., 2021; Xu et al., 2022), but the implementation of such binders to detect endogenously tagged proteins can be challenging due to the stoichiometry of the chromobody relative to the target protein, normally being orders of magnitude larger (Aguilar et al., 2019). We fused the anti-ALFA nanobody to mCherry (hereafter, ALFA-Chromobody) and expressed it in wing imaginal discs using *en*-Gal4 both in absence and presence of the cortically localized Sqh::ALFA:HA (Figure 4B). In both cases, the ALFA-Chromobody totally filled the cytoplasm, rendering the visualization of cortical Sqh::ALFA:HA impossible due to the high background. While dramatic reduction of chromobody levels is possible via titration of the Gal4/UAS expression system, this would be incompatible in many experimental setups. Hence, we decided to engineer the nanobody to be degraded if unbound to its target. To do so, we introduced into the nanobody core the six mutations proposed to result in such behavior (J. C. Tang et al., 2016) (Figure 4A). These mutations destabilized the Chromobody, but did not result in cortical accumulation when co-expressed with Sqh::ALFA:HA (Figure 4B), most likely due to loss of target affinity. The ALFA nanobody partially interacts not only with the ALFA peptide via its CDRs but also with the lateral surface of the core ({Götzke, 2019 #502}, Figure 4A). One of the mutations introduced (R65V) was indeed located on the interacting surface with the ALFA peptide. When the ALFA-Chromobody bearing only the other five mutations was expressed, the Chromobody was still largely unstable in Sqh::ALFA:HA absence, but localized cortically if co-expressed with Sqh::ALFA-HA, indicative of Sqh binding (Figure 4B). Similarly, we generated an ALFA-Chromobody only mutated in the three positions (T75R, C100Y and S124F) predicted to have the largest effect in conditional stability of the nanobody (J. C. Tang et al., 2016) and the smallest in the affinity for the ALFA peptide. This form was slightly less unstable than the 5-mutation version, but it resulted in an increased cortical localization when co-expressed with Sqh::ALFA:HA (Figure 4B).

While protein visualization is critical for many studies, direct protein manipulation is fundamental to assess functional roles. We have previously introduced a method to degrade GFP-tagged peptides via deGradFP, an anti-GFP nanobody fused to an F-box that is able to

recruit the degradative machinery (E. Caussinus, Kanca, & Affolter, 2011). Here, we decided to fuse the ALFA nanobody to the same F-box as deGradFP, aiming to degrade ALFA-tagged proteins (Figure 4C). When degradALFA was expressed in the posterior compartment using *en*-Gal4 in a *sqh*$^{ALFA:HA}$ homozygous background, the protein was dramatically reduced from posterior cells, as detected with an anti-HA antibody (Figure 4D). According to previous deGradFP results (Emmanuel Caussinus & Affolter, 2016; Ochoa-Espinosa, Harmansa, Caussinus, & Affolter, 2017; Pasakarnis, Frei, Caussinus, Affolter, & Brunner, 2016), small non-degraded accumulations were detected in the basal part of the cell. The size and shape of the affected posterior compartment was also perturbed in respect to the anterior.

In addition to degradation of peptides, we foresaw a new method to prevent secretion of proteins tagged with ALFA in the cytoplasmic domain. In this case, we fused the ALFA nanobody to the cytoplasmic tail of CD8. In addition, we added the retention signal KKXX to its C -terminus (Figure 4E). For visualization purposes, CD8 was tagged in the N-terminus with mCherry. We refer to this construct as ALFA-Trap^{ER}. Expression of ALFA-Trap^{ER} using the *pdm2*-Gal4 driver in a *ptc*$^{ALFA:HA}$ background resulted in strong Ptc accumulation as observed using anti-HA antibody (Figure 4F), suggesting impaired secretion.
Together, we present a novel nanobody-based toolbox that permits simultaneous visualization and manipulation of proteins tagged with short peptides in tandem.

Discussion

Here, we have developed a novel strategy to generate knock-ins in Drosophila, namely SEED/Harvest. As other knock-in technologies, SEED relies on the HDR pathway to insert exogenous DNA in the targeted locus. In contrast to other alternatives, CRISPR is also responsible for the removal of the marker used for screening in an SSA-dependent process. Its sole dependency on CRISPR/Cas9, makes SEED a powerful alternative to current methods and opens a series of experimental possibilities. We have demonstrated the versatility of the method by tagging relevant genes of the Hh pathway, thus generating a valuable toolbox for the field. We now use SEED to routinely generate knock-ins and validated its use in several loci, obtaining robust efficiency of insertion and harvesting.

Comparison to other methods

In contrast to most methods, SEED permits scarless tagging of the targeted locus. This feature is fundamental for many purposes, like internal tagging of proteins or the generation of point mutants. In these cases, scars would disrupt the protein sequence in unpredictable ways. Scarless tagging could also be achieved when using templates that do not contain a selectable marker for screening (Port et al., 2014a). These templates permit the generation of scarless knock-ins in one step. However, they require the screening to be performed via PCR, as most of the tagged genes are hardly visible with fluorescence binoculars. While this approach can be used to generate few knock-ins at a time, scaling up seems unfeasible, as it would require extensive labor force. Moreover, efficiency of insertion varies among loci. In this study, the insertion in *shf* locus led to only two founder parents out of 30 fertile F0 individuals (Figure 2H). In that case, PCR screening would have been likely to fail.
To date, PBac technologies also permit rapid screening and scarless marker removal in Drosophila (https://flycrispr.org/ (Nyberg et al., 2020). This technology has demonstrated to

be efficient in many loci. SEED and PBac technologies present several differences. The first is the dependency on a TTAA site. TTAA sites are required to insert the terminal repeats of the PBac transposon. These sites are abundant in introns and other non-coding regions but scarce in exonic sequences. While TTAA sites can be added via silent mutations or included in linker sequences, they generally complicate the cloning or result in insertion of amino acids rarely used in linkers (Chen, Zaro, & Shen, 2013). The second difference strides on the machinery needed for marker removal. The dependency on PBac transposase is not a problem in Drosophila, where many genetic tools have been already stablished. Nevertheless, when applying these technologies in non-model organisms, the SEED solely dependence on CRISPR/Cas turns advantageous. Moreover, expression of transposase entails the risk of transposon insertion in other loci, with potentially unpredictable consequences. Finally, SEED technology can be used in combination with other CRISPR-based tissue specific tools.
The SEED approach also presents inherent limitations in certain set-ups. The most obvious is the integration of highly repeated sequences. In these cases, SSA-mediated removal of the selectable marker is likely to produce many different outcomes; in such cases SEED is not the most suitable alternative.

Ready-to-use reagents

For many laboratories, one of the most time-consuming steps to generate knock-ins is the cloning of donor vectors. Amplification and cloning of long homology arms is many times challenging. One of the main advantages of SEED/Harvest is the simplicity by which donor templates are generated. In this study, we provide reagents to tag genes with common tags used for protein purification and visualization, as well as fluorescent proteins (Figure 1). In addition to these tools, we have adapted the SEED technology to be used with short homology arms (<200bp). Small homology arms had been proven successful for integration of other donors (Kanca et al., 2019). In that line, we did not observe a major decrease in integration efficacy respect long homology arms (Figure 2). Interestingly, our approach yielded a very high integration efficiency, of around 50% (excluding the aforementioned case of *shf).* These rates are higher than those previously described using short homology arms (Kanca et al., 2019). While it is unclear whether these differences are due to the SEED strategy or injection procedure, they highlight the potential of the strategy.
Donors with short homology arms require vector synthesis by a commercial provider and a one-day cloning. For most, this strategy will suffice in time and cost. Nevertheless, we envisioned a way to optimize both. Inspired by previous reports (Wierson et al., 2020), we employed even shorter homology arms to generate donors. This approach permitted one day cloning, without the delay that synthesis implies, while maintaining a considerable efficiency compared to 185bp homology arms (Figure 2L, M). This is the first time this strategy is used in Drosophila and it questions the requirement of the 500bp-1500bp length of homology arms in most CRISPR approaches.

Tissue specific protein labeling.

An intriguing feature of SEED cassettes is the possibility to remove the marker in somatic cells, and therefore induce endogenous tagging. In fact, these insertion cassettes are by-products when generating the scarless knock-in.
Conditional gene labeling has been achieved in the past via careful locus engineering (Alexandre et al., 2014). While yielding very robust results, the applicability of this approach

might be limited in other organisms, given the many generations required to generate these alleles. Recently, several tools based on artificial intron tagging have been proposed to mediate conditional gene labeling via restricted Flippase expression (Fendl, Vieira, & Borst, 2020; Nagarkar-Jaiswal, Manivannan, Zuo, & Bellen, 2017; Williams, Shearin, & Stowers, 2019). These studies provide a valuable asset for many genes where intronic tagging is possible. However, many proteins require internal, N- or C- terminal tagging, which would not be suitable for such a design. In turn, SEED permits gene labeling upon CRISPR-mediated DSB. In the past years, tissue specific expression of Cas9 has been proposed to trigger numerous events, from gene knock-out (Koreman et al., 2021; Meltzer et al., 2019; Port, Chen, Lee, & Bullock, 2014b) to cell (Koreman et al., 2021) and membrane labeling (Garcia-Marques et al., 2019). SEED/Harvest can be easily combined with these to design increasingly complex experiments while reducing the number of tools needed.
CRISPR/Cas9 system requires very low expression levels to function. In that line, we found that somatic harvesting of SEED and CaSSA cassettes are activated mainly at low Cas9 levels (Figure 3B and Supplementary figure 4A). This and previous studies (Koreman et al., 2021; Port et al., 2014b), highlight the necessity to tightly control the Cas9 expression when tissue specific uses of Cas9 are intended.

Protein manipulation using nanobodies
In many cases, the generation of knock-ins pursues the tagging of a protein with a short tag or a fluorescent protein. In this study we propose the tagging with small protein tags in tandem. Recently, we and others have proposed the *in vivo* manipulation of proteins via these short tags, demonstrating that one copy is enough for efficient manipulation (Vigano et al., 2021; Xu et al., 2022). To complement these reagents, we developed a toolbox to visualize and manipulate proteins via the ALFA nanobody (Götzke et al., 2019).
Visualization of proteins through chromobodies depends on a tight balance between the levels of the target protein and the chromobody itself. It has been proposed that many nanobodies are inherently destabilized in absence of antigen (Keller et al., 2018). We found this not to be the case for the ALFA nanobody (Figure 4B). To generate a useful chromobody we rationally engineered the ALFA nanobody to be degraded unless bound. We grafted the mutations proposed to cause conditionally stable behavior (J. C. T. Tang et al., 2016) without much success. In turn, certain combinations of these permitted us the isolation of a functional destabilized chromobody (Figure 4B). The destabilized ALFA nanobody that we present here is the first conditionally unstable nanobody detecting a short tag, with many potential applications in synthetic and basic biology.

Together, these tools permit the robust, affordable and rapid generation of knock-ins, as well as conditional gene tagging, protein visualization and manipulation.

Material and methods

Immunohistochemistry and imaging
3rd instar larvae of the indicated genotype were dissected in cold PBS (PH 7.2, Gibco™ (PN: 20012019)), immediately followed by fixation at room temperature for 30 min using a 4% paraformaldehyde solution (Electron Microscopy Sciences, (PN:15714)) in PBS. After thorough washing with PBS, samples were directly mounted or subjected to

immunohistochemistry. For immunohistochemistry, samples were permeabilized in PBST (PBS + 0,3% Triton X-100 (Sigma PN:1002194227)) for 30 min, followed by 1h incubation in blocking solution (5% Normal Goat Serum (Abcam, ab7481) in PBST). Primary antibodies were diluted in blocking solution and used to incubate samples overnight at 4 degrees. The next day, samples were washed with PBST for 3x15min and incubated for 2 hours in secondary antibody diluted in blocking solution. A final 3x15min washing in PBST and 2x15min washing in PBS was performed before mounting. Samples were gently rotated during fixation and immunostaining. For mounting, samples were placed in Vectashield® with (PN: H-1200) or without DAPI (PN: H-1000). Tissues where then separated from the larval cuticle on a glass slide. A cover-slide was placed on top and sealed with nail polish. Preparations were imaged using LSM880 confocal and analyzed by OMERO and imageJ.

Antibodies used in this study

The following antibodies were used in this study: anti-HA 1/200 (3F10 clone, sigma), anti-Ptc 1/150 (Apa1.3, isolated from hybridoma cells (Capdevila et al., 1994)), 488 conjugated anti-ALFA 1/500 (clone 1G5, Nanotag Biotech.), Alexa fluor 568 anti-Rat (Invitrogen, A11077).

Single fly PCR

Flies were anesthetized with CO2 and placed in PCR tubes on ice. Samples were homogenized using a plastic tip in 30µL of squishing buffer (10mM Tris-HCl, 2.5mM EDTA, 25mM NaCl, 200ng/mL Proteinase K). Following, samples were incubated at 37 degrees for 30min. Proteinase K was subsequently inactivated by heating at 95 degrees for 5min. 1µL was used for downstream PCRs.

Generation of donor vectors

185bp-long homology arms donors were generated by Gibson Assembly of the synthesized vector digested with BbsI and the chosen SEED cassette (see Supplementary figure 2). SEED cassettes were linearized by PCR with primers specific for GFP (P1 and P2) or mCherry (P3 and P4) or by NaeI-SfoI digestion if employing the vectors with short tags in tandem.

Synthesized homology arms were flanked with the gRNA target flanking its sequence to ensure *in vivo* linearization. To permit Gibson Assembly, 30bp complementary to each end of the SEED cassette of choice were added in phase with the homology arms. In between, two Bbs1 cassettes were placed to linearize the vector. Synthesized fragments were cloned into pUC-GW plasmids. All the synthesized fragments are included in the Extended materials. When necessary, silent mutation were introduced to avoid cutting of the donor vectors and/or inserted transgenes. The detailed generation of all plasmids used in this study is included in Table 3 of extended materials.

The 30bp-long homology arm donors were generated by PCR of the pSEED-sfGFP cassette using primers 59 and 60 and subsequent cloning into pBluescript (see Table 2 of extended matherials for primer information and Supplementary figure 2 for the cloning outline). Primers included the gRNA targets for *in vivo* linearization and restriction sites SacI and EcoRI.

Generation of gRNA expressing vectors

gRNAs were cloned into pCFD5 (Addgene 73914) by BbsI digestion and Gibson Assembly as previously described (Port & Bullock, 2016). gRNA targets can be found in Table 1 of extended materials. For gRNAs targeting *ptc* and *sqh*, transgenics were generated using the attP40 landing site (BL 25709).

Generation of harvester stocks

pHarvester was generated using pCFD5-gRNA#1&2 and pnos-Cas9-nos plasmids (Addgene no: 62208). Briefly, the attB site in pnos-Cas9-nos was reversed by SpeI digestion and re-ligation. Subsequently, the attB, gipsy insulator, U6 promoter and gRNA array from pCFD5-gRNA#1&2 were amplified with the primers P5 and P6. Gibson Assembly was used to introduce the amplified fragment into pnos-Cas9-nos vector digested with ApaI and NheI, thus removing the mini-white marker. Harvester stocks were generated via RMCE as described previously (Sun, Johnson, Zeidler, & Bateman, 2012) using the TM3, attP.w[+].attP, Sb, Ser stock (BL 38451).

Fly injection

Fly embryos were injected as follows: 30 min old eggs were dechorionated in 3.5% bleach solution, aligned using a stereomicroscope and adhered on a glass slide. To avoid desiccation, embryos were covered with Voltalef H10S oil. PBS diluted samples were then injected in the posterior pole using a glass needle with the help of a pressure pump and a micromanipulator.
The concentrations employed were: gRNAs plasmids, 100ng/µl; donor vectors, 100ng/µl; injections into attP lines, 300 ng/µl. We used *nos*-Cas9 flies (BL 78782) for all our knock-ins.

List of stocks generated or used in this study

ihog^{sfGFP}	This study
ihog$^{sfGFP\text{-}SEED}$	This study
boi^{mCh}	This study
ptc^{ALFAHA}	This study
sqh^{ALFAHA}	This study
shf^{sfGFP}	This study
ihog^{LOXPSEEDsfGFP}	This study
Dr/TM3,Sb,Ser,Harvester	This study
$w^{[-]}$;M{UAS-sfGFP-SEED, $w^{[+]}$}zh-86Fb	This study
$w^{[-]}$;M{UAS-ALFA-HA-SEED, $w^{[+]}$}zh-86Fb	This study
$y^{[1]}$ $v^{[1]}$; P{U6-gRNA1&2, $v^{[+]}$}attP40	This study
$y^{[1]}$ $v^{[1]}$; P{U6-sqh gRNA 9#, $v^{[+]}$}attP40	This study
$y^{[1]}$ $v^{[1]}$; P{U6-ptc gRNAx2, $v^{[+]}$}attP40	This study
$w^{[-]}$;M{UAS-deGradALFA, $w^{[+]}$}zh-86Fb	This study
$w^{[-]}$;M{UAS-ER-ALFAtrap, $w^{[+]}$}zh-86Fb	This study
$w^{[-]}$;M{UAS-ER-ALFAtrap, $w^{[+]}$}zh-36B	This study
$w^{[-]}$;M{UAS-ALFAWT-mCh, $w^{[+]}$}zh-86Fb	This study

$w^{[-]}$;M{UAS-dALFA6mut-mCh, $w^{[+]}$}zh-86Fb	This study
$w^{[-]}$;M{UAS-dALFA5mut-mCh, $w^{[+]}$}zh-86Fb	This study
$w^{[-]}$;M{UAS-dALFA3mut-mCh, $w^{[+]}$}zh-86Fb	This study
hh-Cas9 (III)	Bloomington number: 81929
*Actin5c*p4.6-IVS-5'mCherry-#2-3'mCherry	Gift from Prof. Tzumin Lee
J28-dU6-3-gRNA(Target#2)	Gift from Prof. Tsumin Lee
nos-Cas9	Bloomington number: 78782
elav-Cas9 (C155)	Bloomington number: 92755
pdm2-Gal4	Bloomington number: 49828

Acknowledgements and founding sources. (~100 words)
We thank Tzumin Lee, Jorge García Marques and the Bloomington stock center for providing fly stocks and sequences used in this study. The work in the laboratory of M.A. was supported by grants from the Swiss National Science Foundation (310030_192659/1) and by funds from the Kanton Basel-Stadt and Basel-Land. GA and MB were supported by 'Fellowships for Excellence' from the International PhD Program in Molecular Life Sciences of the Biozentrum, University of Basel. The work at IG laboratory was supported Grant PID2020-114533GB-C21 to IG and PRE2018-085510 to CJ-J from the Spanish Ministry of Science, Innovation and Universities.

Figure legends.

Figure 1. The SEED/Harvest strategy. A. Outline of the knock-in strategy. pSEED donor plasmids are composed by the following elements: 1) the selectable marker 3xP3-dsRED, 2) targets for two gRNAs with no cutting sites in the fly genome, here denominated 1# and 2# (following the nomenclature of Garcia-Marques et al. 2019), 3) the intended sequence to be inserted in the target locus, this sequence will be split in two parts (3' and 5'), with a common repeat of 100-400 bp, 4) the homology arms to trigger HDR upon DSB formation, and 5) the target sequences of the gRNA that will also cut the genome, flanking the homology arms (here arbitrarily denominated 3#). Upon providing Cas9 and the gRNA 3#, a DSB will be generated in the locus of interest. The DSB will be then repaired by HDR using the highly recombinogenic linearized donor as a template. **B.** Harvesting step. Upon insertion and selection via the 3xP3-dsRED marker, gRNAs 1# and 2# and Cas9 are provided, resulting in the excision of the dsRED marker. Given the presence of the repeats flanking the DSB, SSA will be the preferred repair pathway, leading to the seamless reconstitution of the full-length desired insert. **C.** Schematic representation of the highly conserved steps of SSA repair; 1) 5'-specific strand degradation, 2) Single strand annealing, 3) Resection of overhangs and ligation. **D.** Example of 3xP3-dsRED inserted in one of the knock-ins generated in this study. **E.** Validation of SEED cassettes. UAS-SEED cassettes were combined with harvester chromosomes and then crossed with *Act5c*-Gal4. SEED-sfGFP was scored via GFP fluorescence (n=172), ALFAHA was confirmed by PCR (n=28). In green, animals with correctly rearranged locus, in red, ds-RED positive animals, in grey, animals with not properly rearranged locus. **F.** Schematic representation of the SEED sequence. 3xP3-dsRED is flanked by the target sequences of gRNAs 1# and 2# repeated three times. The basic pSEED plasmid contains 2 MCS to facilitate downstream cloning. Summary of the generated

reagents. Notice the blunt end restriction enzymes (NaeI and SfoI) to liberate SEED for downstream cloning. Asterisk: pSEED-mCherry is marked with 3xP3-GFP to avoid SSA rearrangements between dsRED and mCherry.

Supplementary figure 1. Harvester stocks and fly generation. A. Harvester stock was generated via the insertion of both *nos*-Cas9 and #1&2 into a balancer chromosome via RMCE (Sun et al., 2012). **B.** Genotype of the generated stocks. **C.** Crossing scheme of the experiment of figure 1E. **D.** Crossing scheme for the generation of knock-ins using SEED/Harvest. Most often, nosCas9 embryos are injected with gRNA-expressing vectors and SEED donors. The F0 generation is then crossed with y,w flies. Screening is usually done in larval stages of the F1 generation. After selection, 3xP3-expressing candidates can be crossed with balancers, to maintain the SEED cassette lines, or, crossed with Harvester Balancer stocks. Cas9 is only expressed in the germ cells, making screening of dsRED/harvester candidates possible in the F2. Finally, the F2 is crossed with Balancer flies to establish the knock-in stocks. After this last step, single crosses must be established to avoid mixing of different alleles.

Figure 2. Precise knock-in generation using SEED/Harvest. A. Details of the *ptc* targeting strategy. Two gRNAs targeting the vicinity of the STOP codon were utilized to insert the SEED cassette. Of the fertile descendants, 58% gave raise to dsRED positive animals (n=60). **B.** *sqh* targeting strategy. Only one gRNA was utilized this time. 50% of the fertile descendants were founders (n=8). **C.** Co-staining of Ptc::ALFA:HA with an antiHA antibody and anti-ALFA nanobody. The anterior stripe pattern mimicked previously reported expression (Capdevila et al., 1994). **D.** Anti-ALFA nanobody staining of Sqh::ALFA:HA. Sqh is ubiquitously expressed, with cortical sub-cellular distribution. **E.** Detail of the subapical plane of the wing disc shown in D. The cortical region can be clearly distinguished from the cytoplasm and the membrane region, resulting in ring-shaped pattern. **F, G, H,** Detailed strategy for the targeting of *ihog*, *boi* and *shf*. Both *ihog* and *boi* are targeted in the C-terminal region, while *shf* is targetted in the second exon, between amino acids 60D and 61G. Rates of dsRED insertion: *ihog*: 0.43% (n=28), *boi*: 0.63% (n=35) and *shf*: 0.08 (n=24). **I, J, K.** Patterns of Ihog, Boi and Shf localization in the wing disc after SEED harvesting. Ihog presents its characteristic downregulation along the A-P boundary. Boi is being localized in a characteristic cross pattern and Shf is downregulated in the central part in response to Hh. **L.** Comparison of knock-in efficiency using homology arms of 185bp and 30bp in the *boi* locus. 185bp: 63% (n=25), 30bp 41% (n=39). **M.** Comparison of seamless insertion precision using homology arms of 185bp and 30bp in the *boi* locus. 185bp: 100% (n=10), 30bp 60% (n=10).

Supplementary figure 2. Different cloning strategies to simplify donor plasmid generation. A. Scheme of the synthesis strategy. 1) Synthesis of the vector. 185bp homology arms, flanked by targets for the gRNA were used to generate the genomic DSB (PAM orientation is highlighted in purple). In between, there are two BbsI target sequences to linearize the vector and 30bp sequences homologous to the ends of the sfGFP. If desired, longer linkers or other features can be added in this synthesized vector. 2) After restriction-enzyme-digestion of the synthesized vector, the sfGFP-SEED cassette can be inserted in a one-step Gibson Assembly thanks to the 30bp homology region. **B.** Addition of homology

arms for MHEJ insertion of fragments with ultra-short homology. 1) SEED cassettes are amplified using forward and reverse primers that include 30bp homology arms, targets for the gRNA generation the genomic DSB and a restriction site to subclone it into pBlueScript or similar short vectors. 2) Restriction-ligation cloning into the vector.

Supplementary figure 3. Generation of point mutations. A. Scheme of the *sd* locus and the sequencing of the targeted region in exon 10. gRNAs used to trigger DSB are underlined in black. **B.** pSEED donor plasmid used as a template. The mutation is introduced in the homology arms, that include a repeat of 100bp. Upon HDR, the 3xP3 marker is inserted, flanked by repeated sequences bearing the mutation. **B'.** SSA-mediated harvest leads in the assembly of the repeats, resulting in a locus modified only in the desired nucleotides. **C.** Sanger sequence of the resulting locus, showing the desired mutation (highlighted in red) and the two silent mutations introduced to avoid cutting by the gRNAs.

Figure 3. CRISPR-triggered somatic labeling. A. Outline of the concept. Flies bearing a sfGFP SEED cassette are crossed with strains that contain Cas9 expressed under a tissue-specific promoter and ubiquitously expressed gRNAs. Before cleavage, proteins are labelled with a truncated version of sfGFP. After DSBs are induced, the sfGFP open reading frame is reconstituted, giving rise to a fluorescent sfGFP-tagged protein. **B**. Wing discs of *ihog*$^{\text{SEED-sfGFP}}$, *U6-gRNA#1+2* animals with and without *hh*-Cas9. In absence of Cas9, Ihog protein remains not fluorescent. When *hh*-Cas9 is present, sfGFP can be detected covering most of the surface of the anterior compartment and in clones in the posterior. **C.** Scheme of double membrane and endogenous protein labeling. SEED cassettes can be combined with CaSSA membrane reporters. Both are activated via CRISPR using the same gRNAs. **D.** Detail of a wing disc in which both CAAX-mCherry CaSSa reporter and *ihog*$^{\text{SEED-sfGFP}}$ have been activated using hh-Cas9 and *U6-gRNA#1+2*. **E.** Detail of a basal plane of the same discs as in D. Ihog can be visualized in puncta along filopodia emanating from the CAAX-mCherry-expressing cells. **F.** Adult wing and wing discs of flies bearing *U6-gRNA#1+2* in a hemizygous *shf*$^{\text{SEED-sfGFP}}$ background. The adult wing presents a phenotype that mimics that of null mutants (Glise et al., 2005; Gorfinkiel et al., 2005), with both veins 3 and 4 (marked with asterisk) in close proximity. Notice that no sfGFP expression can be detected as the cassette has not been activated. Both Ptc and Ci155 were only detected in the cells closest to the AP boundary. **G.** Adult wing and wing discs of flies containing *U6-gRNA#1+2* and *hh*-Cas9 in a *shf*$^{\text{SEED-sfGFP}}$ hemizygous background. Note the greater separation between veins 3 and 4 compared to F. sfGFP is now present in the wing disc, resembling the pattern of the *shf*$^{\text{SEED-sfGFP}}$ knock-in (Figure 2K). Both Ptc and Ci155 display an increased range respect compared to respect panels in F. **H.** Quantification of the anti-Ptc signal of panels F and G. **H.** Quantification of the anti-Ci155 signal of panels F and G.

Supplementary figure 4. A. Pattern of the CAAX-mCher(#2)rry CaSSA reporter activation in presence of *hh*-Cas9 and ubiquitously expressed gRNAs #1 and #2. The mCherry signal can be detected covering most of the anterior compartment and in sparse clones in the posterior compartment. **B.** Pattern of *ihog*$^{\text{SEED-sfGFP}}$ activation using only one of the harvesting gRNAs (#2) and *hh*-Cas9. The anterior compartment is mostly covered with little or no clones in the posterior. **C.** Larval VNC of *ihog*$^{\text{SEED-sfGFP}}$ flies combined with *vGlut*-Cas9 and ubiquitously expressed gRNA#2. Ihog labels small structures that resemble somas at the

lateral regions. **D.** Larval VNC of *ihog*$^{\text{SEED-sfGFP}}$ flies combined with *elav*-Cas9 and ubiquitously expressed gRNA#2. Like for *vGlut*-Cas9, somas can be labelled. **D'.** Detail view of some of the somas labelled with Ihog using *elav*-Cas9. **E.** Clones of Ihog-sfGFP expression in the wing disc from the same genotype as in D and D'. **F.** Scheme of the pSEED-LoxP-FP vectors. Two loxPs are inserted flanking the 3xP3-FP marker. **G.** Upon Cre activation, the LoxP sites recombine, removing the 3xP3 marker. The cassette remains sensitive to the activation via both gRNAs #1 and #2. **H.** Percentage of founder 3xP3-dsRED animals using pSEED-Ihog-sfGFP and pSEED-ihog-sfGFP-LoxP. pSEED-Ihog-sfGFP: 43% (n=28), pSEED-ihog-sfGFP-LoxP 42% (n=24).

Figure 4. Protein visualization and manipulation using ALFANb. A. Structure of the ALFANb (yellow) bound to the ALFA peptide (grey) (PBD:2I2G, (Götzke et al., 2019). Substitutions introduced to make it unstable are highlighted in red. Note that R65V is located on the surface contacting ALFA. The 6-mutation version includes all 6 substitutions. The 5-mutation includes all but R65V. The 3-mutation version includes only T75R, C100Y and S124F. **B.** Expression of the different versions of the ALFANb fused to mCherry using *en*-Gal4 in absence (first row) or presence (second row) of endogenously tagged Sqh:ALFA::HA. The WT ALFANb presents similar levels in both presence and absence of Sqh:ALFA:HA, filling the cytoplasm. The 6-mutation version is highly destabilized in absence of Sqh:ALFA::HA, but fails to localize cortically in its presence. The 5-mutation version is still destabilized in Sqh:ALFA:HA absence, but localizes cortically in its presence. The cortical localization was enhanced in the 3-mutation version, amid a slight increase of the levels when Sqh::ALFA:HA was absent. **C.** Scheme of ALFANb-mediated degradation. The ALFANb (in yellow) is fused to the F-box domain contained in the N-terminal part of Slmb. Upon binding of an ALFA-tagged peptide, the F-box recruits the polyubiquitination machinery, targeting the POI to degradation. **D.** Wing discs expressing degradALFA in the posterior compartment (delimited by a dotted line) using the *en*-Gal4 driver. Notice the not-straight shape of AP boundary in the pouch. An apical (left column) and a basal (right column) plane are shown. In green, an immunostaining using anti-ALFANb is displayed. The posterior compartment presents strongly decreased levels compared to anterior compartment, indicating that Sqh levels are reduced, or the ALFA-peptide is masked by the ALFANb. In white, an anti-HA staining of the same discs is shown. The HA signal is also greatly reduced, suggesting decreased Sqh:ALFA:HA levels. Dotted signal can be observed, especially in the basal plane. **E.** Scheme of the ALFA-Trap^{ER}. CD8 is fused to mCherry at its luminal/extracellular region and to ALFANb at its cytoplasmic tail. In addition, KKXX sequence was added in its C-terminus to mediate retention in the ER. If co-expressed with ALFA-tagged transmembrane peptides ALFA-Trap^{ER} can impede its secretion. **F.** Wing discs of *ptc*$^{\textit{ALFA}:\text{HA}}$ flies in absence (first column) or presence (second column) of the ALFA-Trap^{ER}. The mCherry signal is observed in the wing pouch upon ALFA-TRAP^{ER} expression. In green, anti-HA immunostaining, revealing increased levels of Ptc::ALFA:HA in the wing disc.

References.

Aguilar, G., Vigano, M. A., Affolter, M., & Matsuda, S. (2019). Reflections on the use of protein binders to study protein function in developmental biology. *Wiley Interdisciplinary Reviews: Developmental Biology*. doi:10.1002/wdev.356

Alexandre, C., Baena-Lopez, A., & Vincent, J. P. (2014). Patterning and growth control by membrane-tethered wingless. *Nature, 505*(7482), 180-185. doi:10.1038/nature12879

Baena-Lopez, L. A., Alexandre, C., Mitchell, A., Pasakarnis, L., & Vincent, J.-P. (2013). Accelerated homologous recombination and subsequent genome modification in Drosophila. *Development, 140*(23), 4818-4825. doi:10.1242/dev.100933

Bhargava, R., Onyango, D. O., & Stark, J. M. (2016). Regulation of Single-Strand Annealing and its Role in Genome Maintenance. *Trends in Genetics, 32*(9), 566-575. doi:https://doi.org/10.1016/j.tig.2016.06.007

Bilioni, A., Sanchez-Hernandez, D., Callejo, A., Gradilla, A.-C., Ibanez, C., Mollica, E., . . . Guerrero, I. (2013). Balancing Hedgehog, a retention and release equilibrium given by Dally, Ihog, Boi and shifted/DmWif. *Developmental Biology, 376*(2), 198-212. doi:10.1016/j.ydbio.2012.12.013

Bischoff, M., Gradilla, A.-C., Seijo, I., Andres, G., Rodriguez-Navas, C., Gonzalez-Mendez, L., & Guerrero, I. (2013). Cytonemes are required for the establishment of a normal Hedgehog morphogen gradient in Drosophila epithelia. *Nature Cell Biology, 15*(11), 1269-U1240. doi:10.1038/ncb2856

Bollen, Y., Post, J., Koo, B.-K., & Snippert, H. J. G. (2018). How to create state-of-the-art genetic model systems: strategies for optimal CRISPR-mediated genome editing. *Nucleic Acids Research, 46*(13), 6435-6454. doi:10.1093/nar/gky571

Capdevila, J., Estrada, M. P., Sanchezherrero, E., & Guerrero, I. (1994). THE DROSOPHILA SEGMENT POLARITY GENE PATCHED INTERACTS WITH DECAPENTAPLEGIC IN WING DEVELOPMENT. *Embo Journal, 13*(1), 71-82. doi:10.1002/j.1460-2075.1994.tb06236.x

Casas-Tintó, S., Arnés, M., & Ferrús, A. (2017). *Drosophila* enhancer-Gal4 lines show ectopic expression during development. *Royal Society Open Science, 4*(3), 170039. doi:doi:10.1098/rsos.170039

Caussinus, E., & Affolter, M. (2016). deGradFP: A System to Knockdown GFP-Tagged Proteins. In C. Dahmann (Ed.), *Drosophila: Methods and Protocols, 2nd Edition* (Vol. 1478, pp. 177-187).

Caussinus, E., Kanca, O., & Affolter, M. (2011). Fluorescent fusion protein knockout mediated by anti-GFP nanobody. *Nat Struct Mol Biol, 19*(1), 117-121. doi:10.1038/nsmb.2180

Ceccaldi, R., Rondinelli, B., & D'Andrea, A. D. (2016). Repair Pathway Choices and Consequences at the Double-Strand Break. *Trends in Cell Biology, 26*(1), 52-64. doi:https://doi.org/10.1016/j.tcb.2015.07.009

Chen, X., Zaro, J. L., & Shen, W.-C. (2013). Fusion protein linkers: property, design and functionality. *Advanced drug delivery reviews, 65*(10), 1357-1369. doi:10.1016/j.addr.2012.09.039

DeWitt, M. A., Magis, W., Bray, N. L., Wang, T., Berman, J. R., Urbinati, F., . . . Corn, J. E. (2016). Selection-free genome editing of the sickle mutation in human adult hematopoietic stem/progenitor cells. *Science Translational Medicine, 8*(360), 360ra134-360ra134. doi:10.1126/scitranslmed.aaf9336

Fendl, S., Vieira, R. M., & Borst, A. (2020). Conditional protein tagging methods reveal highly specific subcellular distribution of ion channels in motion-sensing neurons. *eLife, 9*, e62953. doi:10.7554/eLife.62953

Garcia-Marques, J., Yang, C.-P., Espinosa-Medina, I., Mok, K., Koyama, M., & Lee, T. (2019). Unlimited Genetic Switches for Cell-Type-Specific Manipulation. *Neuron, 104*(2), 227-238.e227. doi:https://doi.org/10.1016/j.neuron.2019.07.005

Glise, B., Miller, C. A., Crozatier, M., Halbisen, M. A., Wise, S., Olson, D. J., . . . Blair, S. S. (2005). Shifted, the Drosophila ortholog of Wnt inhibitory factor-1, controls the distribution and movement of Hedgehog. *Developmental Cell, 8*(2), 255-266. doi:10.1016/j.devcel.2005.01.003

González-Méndez, L., Seijo-Barandiarán, I., & Guerrero, I. (2017). Cytoneme-mediated cell-cell contacts for Hedgehog reception. *eLife, 6*. doi:10.7554/elife.24045

Gorfinkiel, N., Sierra, J., Callejo, A., Ibanez, C., & Guerrero, I. (2005). The Drosophila ortholog of the human Wnt inhibitor factor Shifted controls the diffusion of lipid-modified Hedgehog. *Developmental Cell, 8*(2), 241-253. doi:10.1016/j.devcel.2004.12.018

Götzke, H., Kilisch, M., Martínez-Carranza, M., Sograte-Idrissi, S., Rajavel, A., Schlichthaerle, T., . . . Frey, S. (2019). The ALFA-tag is a highly versatile tool for nanobody-based bioscience applications. *Nature Communications, 10*(1), 4403. doi:10.1038/s41467-019-12301-7

He, S., Cuentas-Condori, A., & Miller, D. M. (2019). NATF (Native and Tissue-Specific Fluorescence): A Strategy for Bright, Tissue-Specific GFP Labeling of Native Proteins in <em>Caenorhabditis elegans</em&gt. *Genetics, 212*(2), 387. doi:10.1534/genetics.119.302063

Helma, J., Schmidthals, K., Lux, V., Nüske, S., Scholz, A. M., Kräusslich, H.-G., . . . Leonhardt, H. (2012). Direct and Dynamic Detection of HIV-1 in Living Cells. *Plos One, 7*(11), e50026. doi:10.1371/journal.pone.0050026

Horn, C., Jaunich, B., & Wimmer, E. A. (2000). Highly sensitive, fluorescent transformation marker for Drosophila transgenesis. *Development Genes and Evolution, 210*(12), 623-629. doi:10.1007/s004270000111

Huang, J., Zhou, W., Dong, W., Watson, A. M., & Hong, Y. (2009). Directed, efficient, and versatile modifications of the Drosophila genome by genomic engineering. *Proceedings of the National Academy of Sciences, 106*(20), 8284-8289. doi:10.1073/pnas.0900641106

Jinek, M., Chylinski, K., Fonfara, I., Hauer, M., Doudna, J. A., & Charpentier, E. (2012). A Programmable Dual-RNA–Guided DNA Endonuclease in Adaptive Bacterial Immunity. *Science, 337*(6096), 816-821. doi:10.1126/science.1225829

Johnson, R. D., & Jasin, M. (2000). Sister chromatid gene conversion is a prominent double-strand break repair pathway in mammalian cells. *The EMBO Journal, 19*(13), 3398-3407. doi:https://doi.org/10.1093/emboj/19.13.3398

Kamiyama, D., McGorty, R., Kamiyama, R., Kim, M. D., Chiba, A., & Huang, B. (2015). Specification of Dendritogenesis Site in Drosophila aCC Motoneuron by Membrane Enrichment of Pak1 through Dscam1. *Developmental Cell, 35*(1), 93-106. doi:10.1016/j.devcel.2015.09.007

Kamiyama, R., Banzai, K., Liu, P., Marar, A., Tamura, R., Jiang, F., . . . Kamiyama, D. (2021). Cell-type–specific, multicolor labeling of endogenous proteins with split

fluorescent protein tags in Drosophila. *Proceedings of the National Academy of Sciences, 118*(23), e2024690118. doi:10.1073/pnas.2024690118

Kanca, O., Zirin, J., Garcia-Marques, J., Knight, S. M., Yang-Zhou, D., Amador, G., . . . Bellen, H. J. (2019). An efficient CRISPR-based strategy to insert small and large fragments of DNA using short homology arms. *eLife, 8*. doi:10.7554/eLife.51539

Keller, B. M., Maier, J., Secker, K. A., Egetemaier, S. M., Parfyonova, Y., Rothbauer, U., & Traenkle, B. (2018). Chromobodies to Quantify Changes of Endogenous Protein Concentration in Living Cells. *Mol Cell Proteomics, 17*(12), 2518-2533. doi:10.1074/mcp.TIR118.000914

Kim, S.-I., Matsumoto, T., Kagawa, H., Nakamura, M., Hirohata, R., Ueno, A., . . . Woltjen, K. (2018). Microhomology-assisted scarless genome editing in human iPSCs. *Nature Communications, 9*(1), 939. doi:10.1038/s41467-018-03044-y

Koles, K., Yeh, A. R., & Rodal, A. A. (2015). Tissue-specific tagging of endogenous loci in Drosophila melanogaster. *Biology Open, 5*(1), 83-89. doi:10.1242/bio.016089

Koreman, G. T., Xu, Y., Hu, Q., Zhang, Z., Allen, S. E., Wolfner, M. F., . . . Han, C. (2021). Upgraded CRISPR/Cas9 tools for tissue-specific mutagenesis in Drosophila. *Proceedings of the National Academy of Sciences, 118*(14), e2014255118. doi:10.1073/pnas.2014255118

Li, X., Bai, Y., Cheng, X., Kalds, P. G. T., Sun, B., Wu, Y., . . . Zhang, Z. (2018). Efficient SSA-mediated precise genome editing using CRISPR/Cas9. *The FEBS Journal, 285*(18), 3362-3375. doi:https://doi.org/10.1111/febs.14626

Lindsley, D. L., & Zimm, G. G. (1992). GENES. In D. L. Lindsley & G. G. Zimm (Eds.), *The Genome of Drosophila Melanogaster* (pp. 1-803). San Diego: Academic Press.

Mao, Z., Bozzella, M., Seluanov, A., & Gorbunova, V. (2008). Comparison of nonhomologous end joining and homologous recombination in human cells. *DNA Repair, 7*(10), 1765-1771. doi:https://doi.org/10.1016/j.dnarep.2008.06.018

Meltzer, H., Marom, E., Alyagor, I., Mayseless, O., Berkun, V., Segal-Gilboa, N., . . . Schuldiner, O. (2019). Tissue-specific (ts)CRISPR as an efficient strategy for in vivo screening in Drosophila. *Nature Communications, 10*(1), 2113. doi:10.1038/s41467-019-10140-0

Mesrouze, Y., Aguilar, G., Meyerhofer, M., Bokhovchuk, F., Zimmermann, C., Fontana, P., . . . Chène, P. (2022). The role of lysine palmitoylation/myristoylation in the function of the TEAD transcription factors. *Scientific Reports, 12*(1), 4984. doi:10.1038/s41598-022-09127-7

Nagarkar-Jaiswal, S., Manivannan, S. N., Zuo, Z., & Bellen, H. J. (2017). A cell cycle-independent, conditional gene inactivation strategy for differentially tagging wild-type and mutant cells. *eLife, 6*, e26420. doi:10.7554/eLife.26420

Nakade, S., Tsubota, T., Sakane, Y., Kume, S., Sakamoto, N., Obara, M., . . . Suzuki, K.-i. T. (2014). Microhomology-mediated end-joining-dependent integration of donor DNA in cells and animals using TALENs and CRISPR/Cas9. *Nature Communications, 5*(1), 5560. doi:10.1038/ncomms6560

Nyberg, K. G., Nguyen, J. Q., Kwon, Y.-J., Blythe, S., Beitel, G. J., & Carthew, R. (2020). A pipeline for precise and efficient genome editing by sgRNA-Cas9 RNPs in Drosophila. *Fly, 14*(1-4), 34-48. doi:10.1080/19336934.2020.1832416

Ochoa-Espinosa, A., Harmansa, S., Caussinus, E., & Affolter, M. (2017). Myosin II is not required for Drosophila tracheal branch elongation and cell intercalation. *Development, 144*(16), 2961-2968. doi:10.1242/dev.148940

Panza, P., Maier, J., Schmees, C., Rothbauer, U., & Soellner, C. (2015). Live imaging of endogenous protein dynamics in zebrafish using chromobodies. *Development, 142*(10), 1879-1884. doi:10.1242/dev.118943

Park, S. H., Lee, C. M., Dever, D. P., Davis, T. H., Camarena, J., Srifa, W., . . . Bao, G. (2019). Highly efficient editing of the β-globin gene in patient-derived hematopoietic stem and progenitor cells to treat sickle cell disease. *Nucleic Acids Research, 47*(15), 7955-7972. doi:10.1093/nar/gkz475

Pasakarnis, L., Frei, E., Caussinus, E., Affolter, M., & Brunner, D. (2016). Amnioserosa cell constriction but not epidermal actin cable tension autonomously drives dorsal closure. *Nature Cell Biology, 18*(11), 1161-+. doi:10.1038/ncb3420

Port, F., & Bullock, S. L. (2016). Augmenting CRISPR applications in Drosophila with tRNA-flanked sgRNAs. *Nature Methods, 13*(10), 852-854. doi:10.1038/nmeth.3972

Port, F., Chen, H.-M., Lee, T., & Bullock, S. L. (2014a). Optimized CRISPR/Cas tools for efficient germline and somatic genome engineering in <em>Drosophila</em&gt. *Proceedings of the National Academy of Sciences, 111*(29), E2967. doi:10.1073/pnas.1405500111

Port, F., Chen, H.-M., Lee, T., & Bullock, S. L. (2014b). Optimized CRISPR/Cas tools for efficient germline and somatic genome engineering in Drosophila. *Proceedings of the National Academy of Sciences, 111*(29), E2967-E2976. doi:10.1073/pnas.1405500111

Port, F., Strein, C., Stricker, M., Rauscher, B., Heigwer, F., Zhou, J., . . . Boutros, M. (2020). A large-scale resource for tissue-specific CRISPR mutagenesis in Drosophila. *eLife, 9*, e53865. doi:10.7554/eLife.53865

Preston, C. R., Engels, W., & Flores, C. (2002). Efficient Repair of DNA Breaks in Drosophila: Evidence for Single-Strand Annealing and Competition With Other Repair Pathways. *Genetics, 161*(2), 711-720. Retrieved from https://www.genetics.org/content/genetics/161/2/711.full.pdf

Roberts, B., Hendershott, M. C., Arakaki, J., Gerbin, K. A., Malik, H., Nelson, A., . . . Gunawardane, R. N. (2019). Fluorescent Gene Tagging of Transcriptionally Silent Genes in hiPSCs. *Stem Cell Reports, 12*(5), 1145-1158. doi:https://doi.org/10.1016/j.stemcr.2019.03.001

Sakuma, T., Nakade, S., Sakane, Y., Suzuki, K.-I. T., & Yamamoto, T. (2016). MMEJ-assisted gene knock-in using TALENs and CRISPR-Cas9 with the PITCh systems. *Nature Protocols, 11*(1), 118-133. doi:10.1038/nprot.2015.140

Sanchez-Hernandez, D., Sierra, J., Ramalho Ortigao-Farias, J., & Guerrero, I. (2012). The WIF domain of the human and Drosophila Wif-1 secreted factors confers specificity for Wnt or Hedgehog. *Development, 139*(20), 3849-3858. doi:10.1242/dev.080028

Simon, E., Jiménez-Jiménez, C., Seijo-Barandiarán, I., Aguilar, G., Sánchez-Hernández, D., Aguirre-Tamaral, A., . . . Guerrero, I. (2021). Glypicans define unique roles for the Hedgehog co-receptors boi and ihog in cytoneme-mediated gradient formation. *eLife, 10*, e64581. doi:10.7554/eLife.64581

Smithies, O., Gregg, R. G., Boggs, S. S., Koralewski, M. A., & Kucherlapati, R. S. (1985). Insertion of DNA sequences into the human chromosomal β-globin locus by homologous recombination. *Nature, 317*(6034), 230-234. doi:10.1038/317230a0

Sun, F. F., Johnson, J. E., Zeidler, M. P., & Bateman, J. R. (2012). Simplified Insertion of Transgenes Onto Balancer Chromosomes via Recombinase-Mediated Cassette Exchange. *G3 Genes|Genomes|Genetics, 2*(5), 551-553. doi:10.1534/g3.112.002097

Tang, J. C., Drokhlyansky, E., Etemad, B., Rudolph, S., Guo, B., Wang, S., . . . Cepko, C. L. (2016). Detection and manipulation of live antigen-expressing cells using conditionally stable nanobodies. *eLife, 5*. doi:10.7554/eLife.15312

Tang, J. C. T., Drokhlyansky, E., Etemad, B., Rudolph, S., Guo, B., Wang, S., . . . Cepko, C. L. (2016). Detection and manipulation of live antigen-expressing cells using conditionally stable nanobodies. *eLife, 5*(MAY2016). doi:10.7554/eLife.15312

Vigano, M. A., Ell, C. M., Kustermann, M. M. M., Aguilar, G., Matsuda, S., Zhao, N., . . . Pyrowolakis, G. (2021). Protein manipulation using single copies of short peptide tags in cultured cells and in Drosophila melanogaster. *Development, 148*(6). doi:10.1242/dev.191700

Wierson, W. A., Welker, J. M., Almeida, M. P., Mann, C. M., Webster, D. A., Torrie, M. E., . . . Essner, J. (2020). Efficient targeted integration directed by short homology in zebrafish and mammalian cells. *eLife, 9*, e53968. doi:10.7554/eLife.53968

Williams, J. L., Shearin, H. K., & Stowers, R. S. (2019). Conditional Synaptic Vesicle Markers for Drosophila. *G3 Genes|Genomes|Genetics, 9*(3), 737-748. doi:10.1534/g3.118.200975

Xu, J., Kim, A.-R., Cheloha, R. W., Fischer, F. A., Li, J. S. S., Feng, Y., . . . Perrimon, N. (2022). Protein visualization and manipulation in Drosophila through the use of epitope tags recognized by nanobodies. *eLife, 11*, e74326. doi:10.7554/eLife.74326

Yan, D., Wu, Y., Yang, Y., Belenkaya, T. Y., Tang, X., & Lin, X. (2010). The cell-surface proteins Dally-like and Ihog differentially regulate Hedgehog signaling strength and range during development. *Development (Cambridge, England), 137*(12), 2033-2044. doi:10.1242/dev.045740

Yao, X., Zhang, M., Wang, X., Ying, W., Hu, X., Dai, P., . . . Yang, H. (2018). Tild-CRISPR Allows for Efficient and Precise Gene Knockin in Mouse and Human Cells. *Developmental Cell, 45*(4), 526-536.e525. doi:https://doi.org/10.1016/j.devcel.2018.04.021

Ye, L., Wang, J., Beyer, A. I., Teque, F., Cradick, T. J., Qi, Z., . . . Kan, Y. W. (2014). Seamless modification of wild-type induced pluripotent stem cells to the natural CCR5Δ32 mutation confers resistance to HIV infection. *Proceedings of the National Academy of Sciences, 111*(26), 9591-9596. doi:10.1073/pnas.1407473111

Yusa, K. (2013). Seamless genome editing in human pluripotent stem cells using custom endonuclease–based gene targeting and the piggyBac transposon. *Nature Protocols, 8*(10), 2061-2078. doi:10.1038/nprot.2013.126

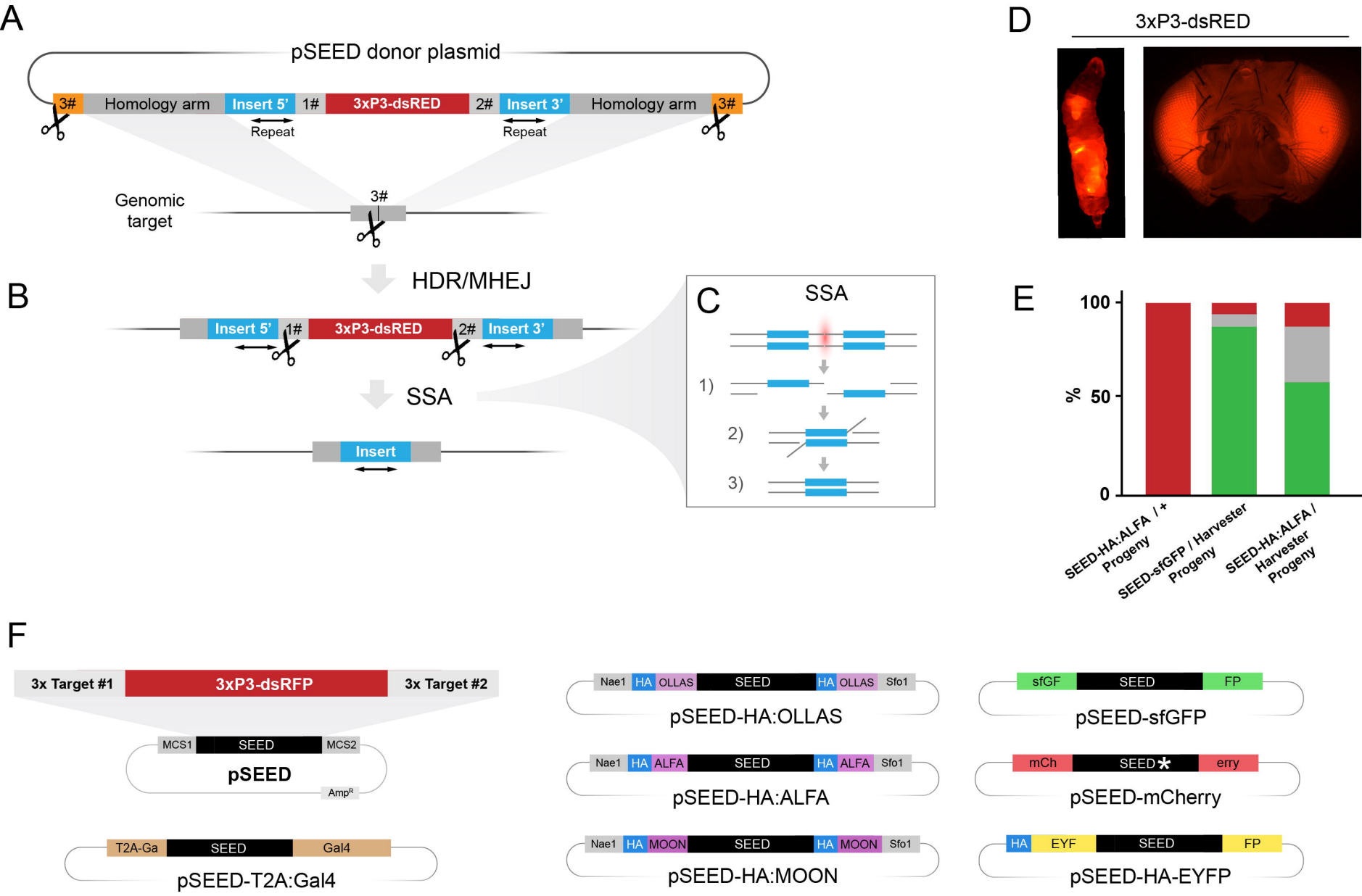
A
pSEED donor plasmid
3#
Homology arm
Insert 5'
1#
3xP3-dsRED
2#
Insert 3'
Homology arm
3#
Repeat
Repeat
Genomic target
3#
HDR/MHEJ
B
Insert 5'
1#
3xP3-dsRED
2#
Insert 3'
SSA
Insert
C
SSA
1)
2)
3)
D
3xP3-dsRED
E
100
50
0
%
SEED-HA:ALFA / +
Progeny
SEED-sfGFP / Harvester
Progeny
SEED-HA:ALFA /
Harvester
Progeny
F
3x Target #1
3xP3-dsRFP
3x Target #2
MCS1
SEED
MCS2
pSEED
Amp^R
T2A-Ga
SEED
Gal4
pSEED-T2A:Gal4
Nae1
HA
OLLAS
SEED
HA
OLLAS
Sfo1
pSEED-HA:OLLAS
Nae1
HA
ALFA
SEED
HA
ALFA
Sfo1
pSEED-HA:ALFA
Nae1
HA
MOON
SEED
HA
MOON
Sfo1
pSEED-HA:MOON
sfGF
SEED
FP
pSEED-sfGFP
mCh
SEED*
erry
pSEED-mCherry
HA
EYF
SEED
FP
pSEED-HA-EYFP

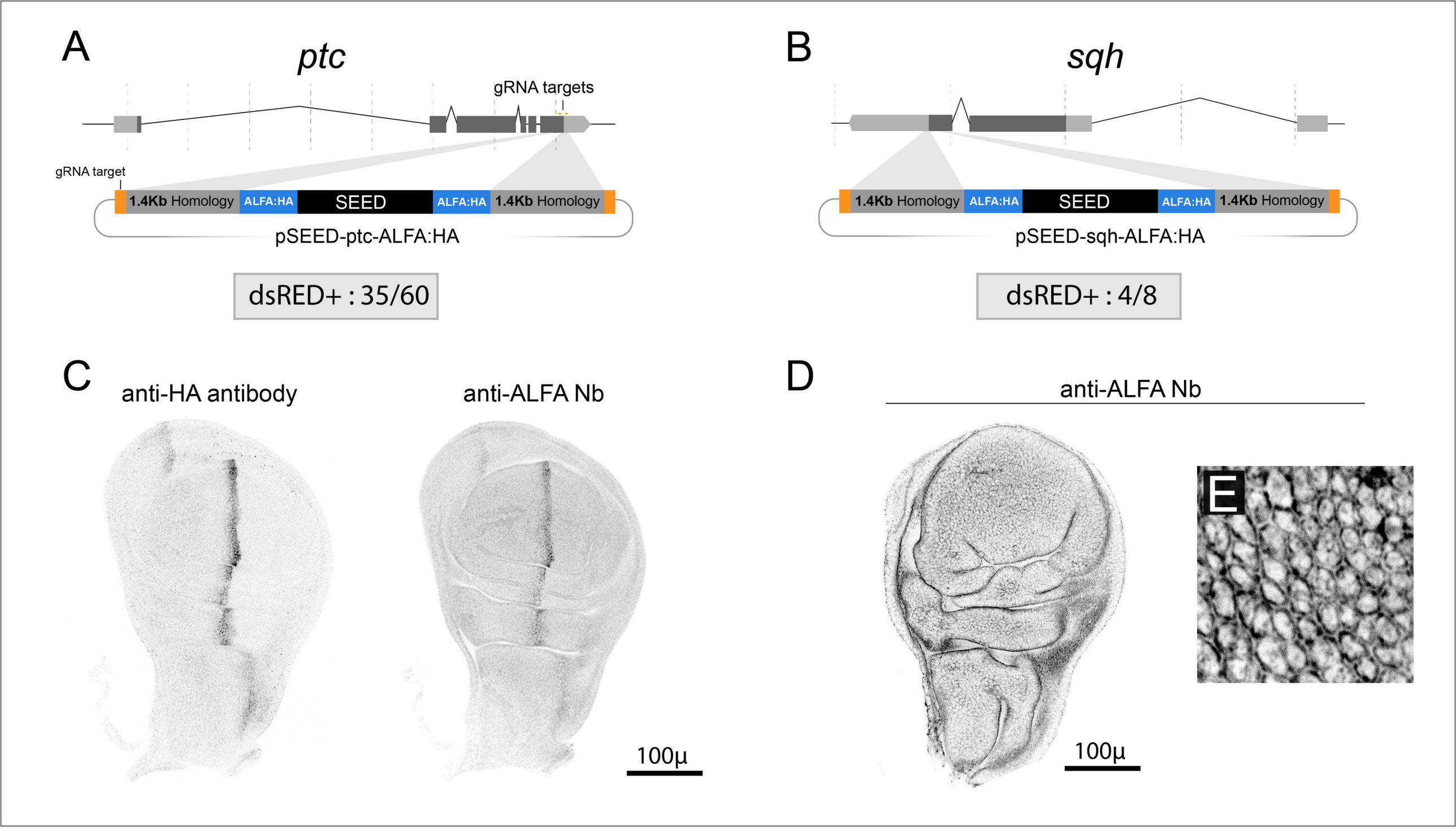
A
ptc
gRNA targets
gRNA target
1.4Kb Homology
ALFA:HA
SEED
ALFA:HA
1.4Kb Homology
pSEED-ptc-ALFA:HA
dsRED+ : 35/60
B
sqh
1.4Kb Homology
ALFA:HA
SEED
ALFA:HA
1.4Kb Homology
pSEED-sqh-ALFA:HA
dsRED+ : 4/8
C
anti-HA antibody
anti-ALFA Nb
100µ
D
anti-ALFA Nb
100µ
E

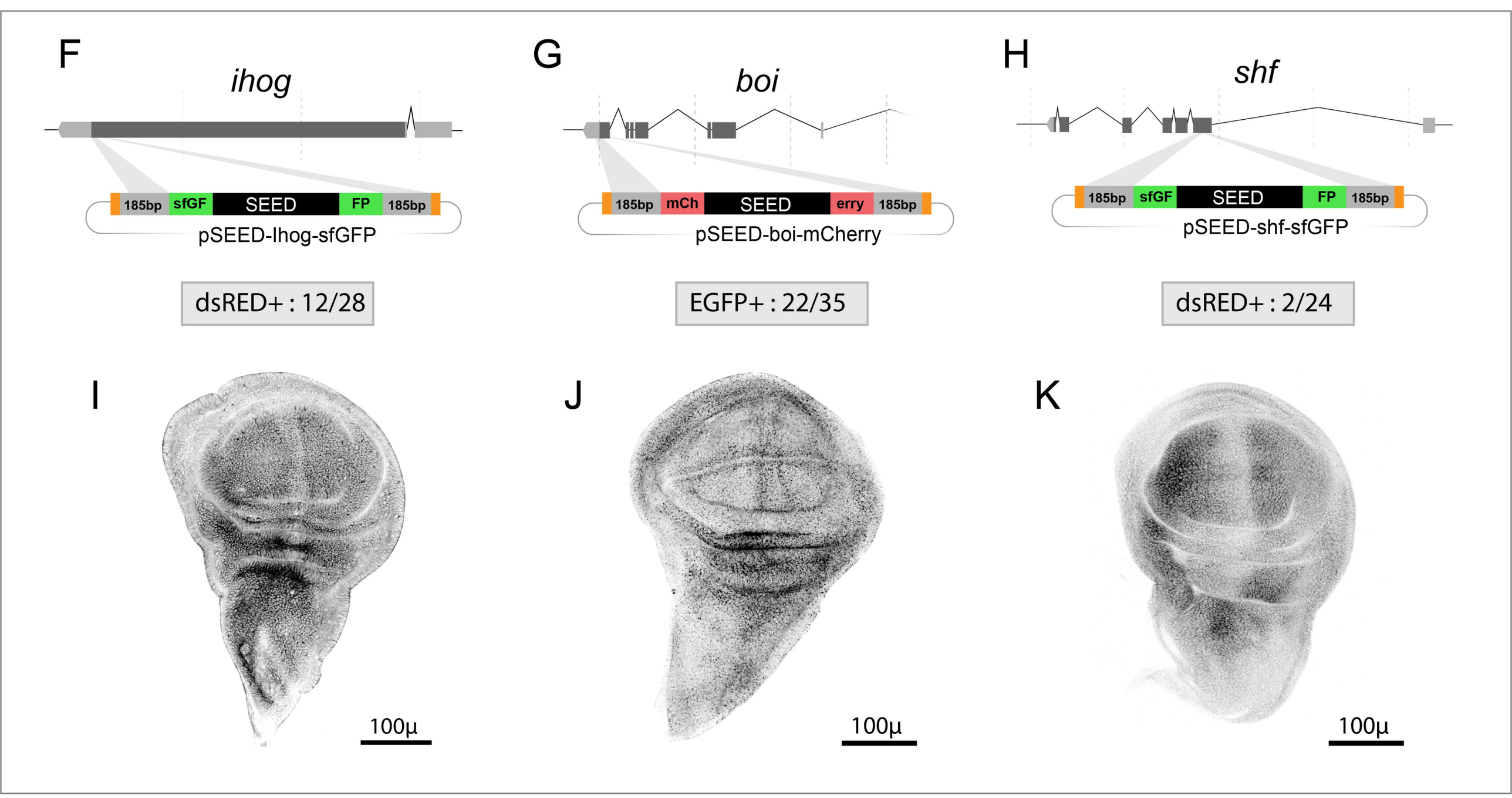
F
ihog
185bp
sfGF
SEED
FP
185bp
pSEED-Ihog-sfGFP
dsRED+ : 12/28
G
boi
185bp
mCh
SEED
erry
185bp
pSEED-boi-mCherry
EGFP+ : 22/35
H
shf
185bp
sfGF
SEED
FP
185bp
pSEED-shf-sfGFP
dsRED+ : 2/24
I
100µ
J
100µ
K
100µ

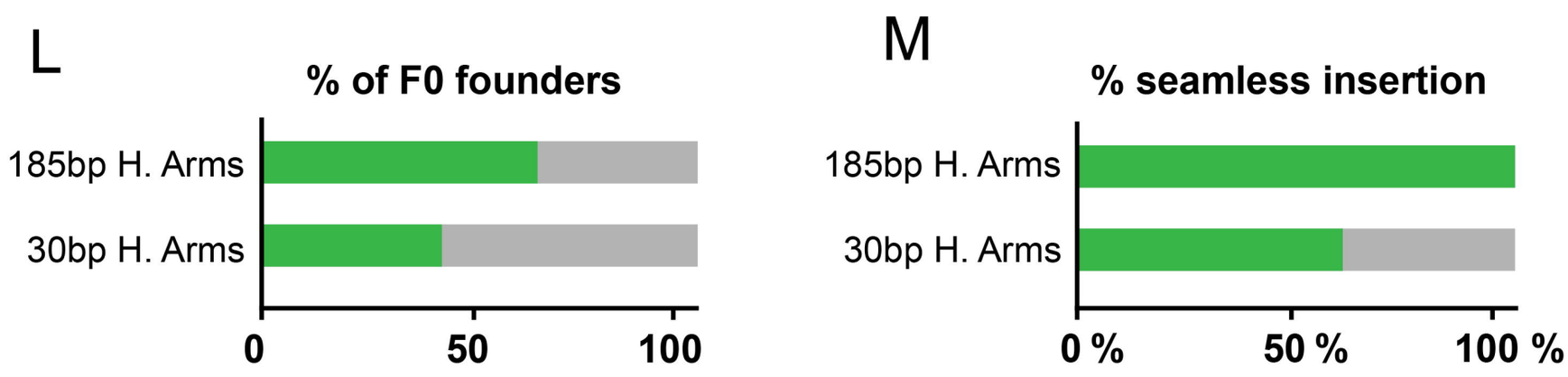
L
% of F0 founders
185bp H. Arms
30bp H. Arms
0
50
100
M
% seamless insertion
185bp H. Arms
30bp H. Arms
0 %
50 %
100 %

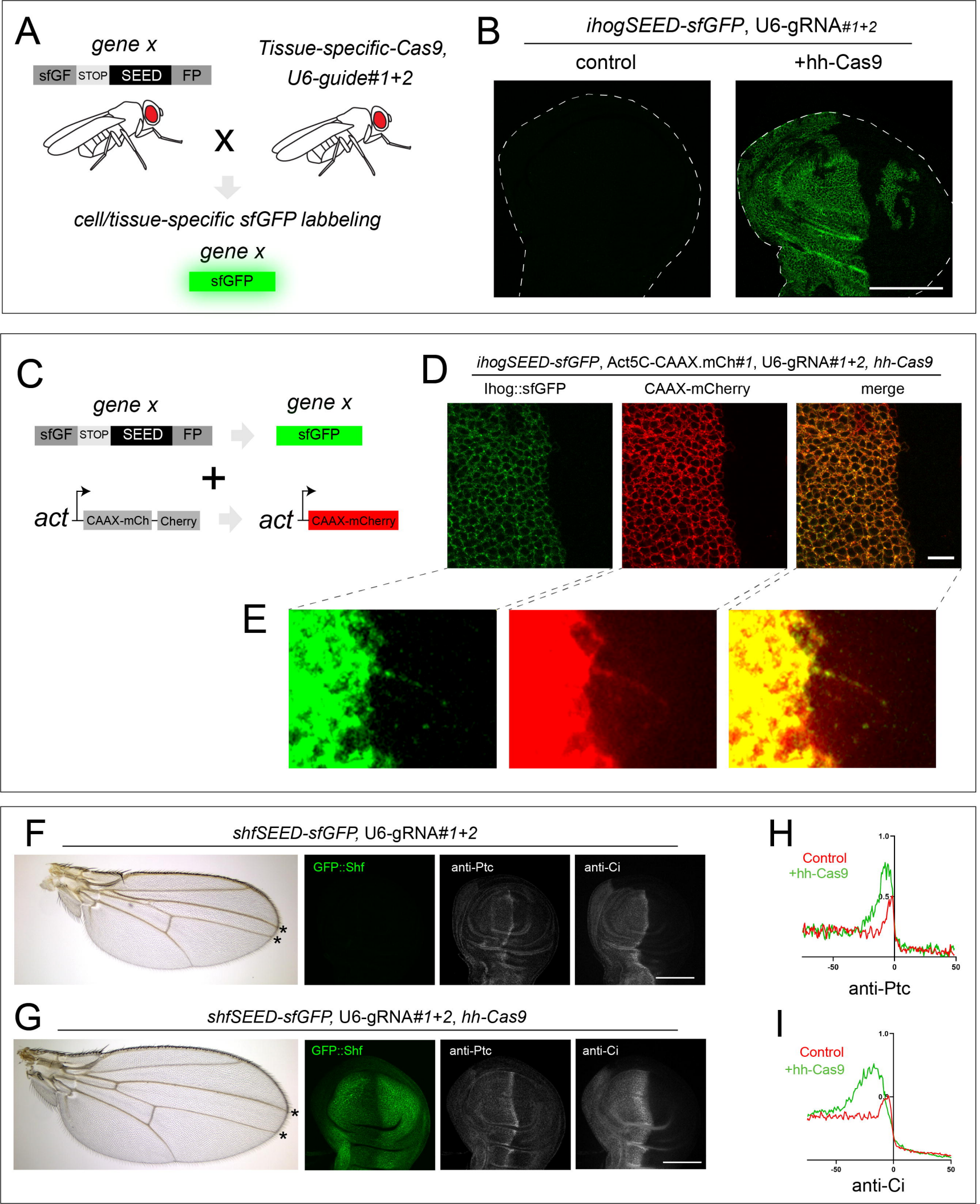
A
gene x
sfGF
STOP
SEED
FP
Tissue-specific-Cas9,
U6-guide#1+2
x
cell/tissue-specific sfGFP labbeling
gene x
sfGFP
B
ihogSEED-sfGFP, U6-gRNA#1+2
control
+hh-Cas9
C
gene x
sfGF
STOP
SEED
FP
gene x
sfGFP
+
act
CAAX-mCh
Cherry
act
CAAX-mCherry
D
ihogSEED-sfGFP, Act5C-CAAX.mCh#1, U6-gRNA#1+2, hh-Cas9
Ihog::sfGFP
CAAX-mCherry
merge
E
F
shfSEED-sfGFP, U6-gRNA#1+2
GFP::Shf
anti-Ptc
anti-Ci
G
shfSEED-sfGFP, U6-gRNA#1+2, hh-Cas9
GFP::Shf
anti-Ptc
anti-Ci
H
Control
+hh-Cas9
1.0
0.5
-50
0
50
anti-Ptc
I
Control
+hh-Cas9
1.0
0.5
-50
0
50
anti-Ci

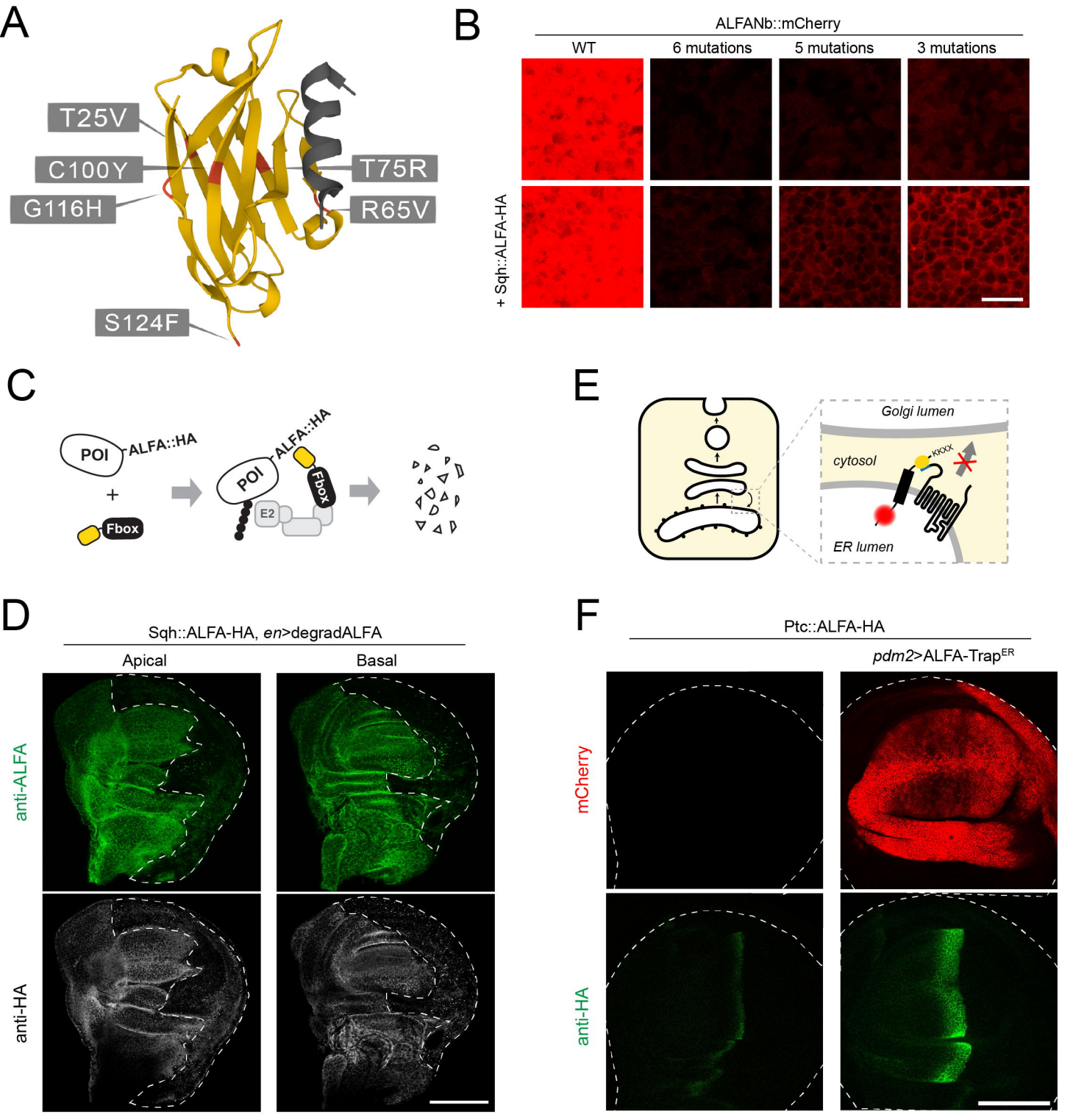
A
T25V
C100Y
G116H
S124F
T75R
R65V
B
ALFANb::mCherry
WT
6 mutations
5 mutations
3 mutations
+ Sqh::ALFA-HA
C
POI
ALFA::HA
+
Fbox
POI
ALFA::HA
Fbox
E2
E
Golgi lumen
cytosol
KKXX
ER lumen
D
Sqh::ALFA-HA, en>degradALFA
Apical
Basal
anti-ALFA
anti-HA
F
Ptc::ALFA-HA
pdm2>ALFA-TrapER
mCherry
anti-HA